

Stochastic surface walking reaction sampling for resolving heterogeneous catalytic reaction network: A revisit to the mechanism of water-gas shift reaction on Cu

Xiao-Jie Zhang, Cheng Shang, and Zhi-Pan Liu

Citation: *The Journal of Chemical Physics* **147**, 152706 (2017); doi: 10.1063/1.4989540

View online: <http://dx.doi.org/10.1063/1.4989540>

View Table of Contents: <http://aip.scitation.org/toc/jcp/147/15>

Published by the [American Institute of Physics](#)



**COMPLETELY
REDESIGNED!**

**PHYSICS
TODAY**

Physics Today Buyer's Guide
Search with a purpose.

Stochastic surface walking reaction sampling for resolving heterogeneous catalytic reaction network: A revisit to the mechanism of water-gas shift reaction on Cu

Xiao-Jie Zhang, Cheng Shang, and Zhi-Pan Liu^{a)}

Collaborative Innovation Center of Chemistry for Energy Material, Key Laboratory of Computational Physical Science (Ministry of Education), Shanghai Key Laboratory of Molecular Catalysis and Innovative Materials, Department of Chemistry, Fudan University, Shanghai 200433, China

(Received 7 May 2017; accepted 8 June 2017; published online 28 June 2017)

Heterogeneous catalytic reactions on surface and interfaces are renowned for ample intermediate adsorbates and complex reaction networks. The common practice to reveal the reaction mechanism is via theoretical computation, which locates all likely transition states based on the pre-guessed reaction mechanism. Here we develop a new theoretical method, namely, stochastic surface walking (SSW)-Cat method, to resolve the lowest energy reaction pathway of heterogeneous catalytic reactions, which combines our recently developed SSW global structure optimization and SSW reaction sampling. The SSW-Cat is automated and massively parallel, taking a rough reaction pattern as input to guide reaction search. We present the detailed algorithm, discuss the key features, and demonstrate the efficiency in a model catalytic reaction, water-gas shift reaction on Cu(111) ($\text{CO} + \text{H}_2\text{O} \rightarrow \text{CO}_2 + \text{H}_2$). The SSW-Cat simulation shows that water dissociation is the rate-determining step and formic acid (HCOOH) is the kinetically favorable product, instead of the observed final products, CO_2 and H_2 . It implies that CO_2 and H_2 are secondary products from further decomposition of HCOOH at high temperatures. Being a general purpose tool for reaction prediction, the SSW-Cat may be utilized for rational catalyst design via large-scale computations. *Published by AIP Publishing.* [<http://dx.doi.org/10.1063/1.4989540>]

I. INTRODUCTION

Reactivity prediction is a main theme in chemistry. Among various types of chemical reactions, heterogeneous catalytic reactions occurring on surfaces and interfaces, e.g., ammonia synthesis on Fe catalysts,¹ rank top in their complexity, where (multiple) chemical bonds of molecules break and form consecutively with the help of solid catalysts. Compared to organic chemistry in solution, the current understanding for heterogeneous reactions is much poorer, not least because of the lack of knowledge on the reaction intermediates, often unsaturated molecular fragments, that are very unstable in the gas phase but turn out to well chemisorb on catalysts.² Since the type and stability of reaction intermediates vary sensitively upon catalysts, the building of the knowledgebase for heterogeneous reaction has been slow and often case-wise, which hinders practically the rational design of novel heterogeneous catalytic reactions.^{3,4}

By combining with geometry optimization, transition state (TS) searching, and enhanced sampling methods, quantum mechanics electronic structure calculations provide an attractive alternative to probe the chemical reactivity, as practiced widely in recent years, ranging from gas phase reactions, to homogeneous catalysis, and to heterogeneous catalysis.^{5,6} The key task in computational studies is to identify the lowest energy reaction pathway in a reaction network [see Fig. 1(a)],

which should dictate largely the reactivity according to the kinetics theory. For heterogeneous reactions that occur often above ambient temperatures, the overall reaction barrier (in the rate-determining step) is high (e.g., >0.7 eV), and a group of reaction intermediates are likely with similar thermodynamic stability. Because the number of reaction pathways increases exponentially with the increase of the number of reaction intermediates,⁷ heterogeneous catalytic reaction often features with a complex reaction network and the search for the lowest reaction pathway becomes time-consuming and highly problematic. The manual way to locate each likely TS by the TS searching method (e.g., dimer method,⁸ nudged elastic band method,⁹ constrained minimization,¹⁰ and constrained Broyden dimer method¹¹) has been popularly practiced, which not only is highly computational demanding but also requires huge labor work for pre-guessing and configuring intermediate (including TS) structures.

To identify automatically the lowest energy reaction pathway, many elegant methods have been developed in the past 20 years. By adding bias along the predefined reaction coordinate, biased molecular dynamics, including umbrella sampling and metadynamics,¹² are often utilized to establish the free energy profile of a given elementary reaction. They are generally not suitable for resolving a complex reaction network with different reaction coordinates. The other class of methods, such as discrete path sampling (DPS)¹³ and minimum-hopping guided pathway search,¹⁴ relies on the double-ended TS searching method to identify the pathway between minima on the potential energy surface (PES) and

^{a)}Email: zpliu@fudan.edu.cn

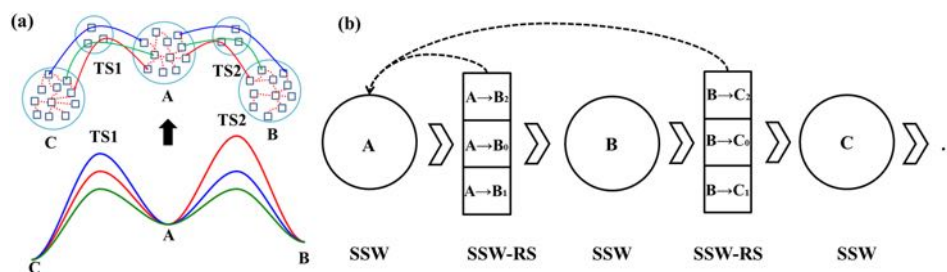


FIG. 1. (a) Schematic reaction network in a two-step, three-minimum (A, B, and C) reaction. For each minimum, as represented by the large circle, there are many possible conformation isomers where the transition between them is rapid. As many likely pathways linking between minima are present, the challenge to theory is finding the lowest energy pathway (the green curve). (b) Flow chart for the SSW-Cat method, which combines SSW for global structure search and SSW-RS for reaction search. In SSW as illustrated by the large circles, the conformation space of reactants (A, B and C) is searched, where a Metropolis Monte Carlo algorithm is used for structure selection. In SSW-RS as illustrated by the rectangle groups, the reaction space for the current reactant is explored, and the occurring of chemical reaction is monitored and recorded as indicated by the reaction formula inside each rectangle.

the kinetics approach (e.g., the graph transformation¹⁵ and the kinetics Monte Carlo¹⁶) to resolve the lowest energy (fastest) reaction pathway. While these methods are highly automated, the computational cost to build a database with all distinct minima and all their connections (pathways) is excessively high, and thus they have been mainly applied in model systems, such as Lennard-Jones particles and small water clusters with TIP4P force fields.⁷ In recent years, Maeda and Morokuma *et al.* developed an artificial force induced reaction (AFIR) method²⁹ for investigating molecular reactions in the gas phase and solution by enforcing reaction to occur on randomly selected atomic pairs.^{17,18} AFIR utilizes exhaustive random configuration generation¹⁹ to construct an ensemble of all reactant configurations, which becomes increasingly difficult for reactions under complex conditions (with huge configuration space), such as those occurring on surfaces and in solid/liquid interface.

The other knowledge-based approaches have also been proposed in recent years, such as reaction mechanism generators, Reaction Mechanism Generation for heterogeneous catalysis (RMG-CAT),²⁰ and Rule Input Network Generator (RING).²¹ These methods can generate a plausible reaction pathway given a set of predefined empirical rules. The computation efforts are spent only on minimum structures, and the transition states along the lowest energy pathway are not calculated accurately.

To date, to identify the lowest energy pathway of heterogeneous catalytic reaction in an automated and efficient way remains as an open challenge. To achieve this goal, two difficult tasks must be fulfilled first: (i) to explore the configuration space of adsorbates, including reactants and intermediates. Since the diffusion of adsorbates is often fast compared to (bond breaking/making) reactions, there are considerable number of molecular adsorption geometries, which are accessible precursor states for reaction to occur; (ii) to identify the correct TS geometry involving bond breaking/making on surfaces. For catalytic reaction, a right TS geometry is critical to lower the reaction barrier, and thus an efficient sampling on the reaction space is a must.

In 2013, our group developed a new global optimization method, namely, the *Stochastic Surface Walking* (SSW) method.^{22,23} The SSW method combines the bias-potential driven structure optimization and Metropolis Monte Carlo

sampling for structure selection, targeting for a rapid potential energy surface (PES) exploration via smooth structure perturbation. In addition to global optimization, the SSW method with a modified structure selection module turns out to be an efficient tool for reaction sampling, i.e., the SSW reaction sampling (SSW-RS).²⁴ In combination with density functional theory (DFT) calculations, the SSW-RS method has been utilized to explore unbiasedly short reaction pathways in different systems, ranging from molecular reactions in the gas phase,^{23,25,26} to surface reconstruction,²⁷ and to solid phase transitions.²⁸

Here we design an automated method for resolving the heterogeneous catalytic reaction network, namely, the SSW-Cat method, by exploiting the functionalities of SSW and SSW-RS. The current SSW-Cat method aims to achieve the efficient PES sampling on both the configurational space of reactants/intermediates and the reaction space containing various TSs. It is able to figure out the lowest energy pathway automatically for a multiple-step reaction process and in the meantime identify the likely (higher energy) by-products and their pathways.

II. METHODOLOGY AND CALCULATION SETUPS

A. SSW and SSW-RS

The new SSW-Cat method carried out alternatively SSW for global structure exploration and SSW-RS for reaction pathway identification [see Fig. 1(b)]. To be more specific, SSW is intended to find new minima corresponding to new/different chemical states; SSW-RS is intended to find new minima corresponding to a particular chemical state as well as possible products of reactions from this chemical state. The algorithms of SSW and SSW-RS methods have been described in detail previously.^{22,24,29} For the flow and clarity of the work, we summarize briefly the key features of SSW and SSW-RS.

1. SSW method

The SSW method^{22,23} has an automated climbing mechanism to manipulate a structure configuration from minimum \mathbf{R}^0 to high-energy configuration \mathbf{R}^H along one random mode direction \mathbf{N}_0 , following the idea of bias-potential driven constrained-Broyden-dimer (BP-CBD) method for TS

location.⁶ The further optimization of the high-energy configuration \mathbf{R}^H will lead to a new minimum \mathbf{R}^I , i.e., one SSW step from \mathbf{R}^0 to \mathbf{R}^I . A structure selection module based on Metropolis Monte Carlo algorithm is applied to decide whether to accept the new minimum according to Eq. (1). By repeating the procedure, one can explore the whole PES and identify new structures unbiasedly. The method has been utilized to identify the global minimum of boron and Pt clusters and explore the global PES of solids (SiO_2),^{26,30,31}

$$P_{mc} = \begin{cases} \exp\left[\frac{E(\mathbf{R}^0) - E(\mathbf{R}^I)}{kT}\right], & \text{when } E(\mathbf{R}^0) > E(\mathbf{R}^I) \\ 1, & \text{otherwise} \end{cases} \quad (1)$$

The initial random mode \mathbf{N}_0 in each SSW step is combined from two random vectors, \mathbf{N}_g and \mathbf{N}_l . \mathbf{N}_g represents a global mode by randomly displacing all atoms in the structure [Eq. (2)]; \mathbf{N}_l is a local mode, for example, as written in Eq. (3) for a mode to drag close two randomly selected A and B atoms with Cartesian coordinates \mathbf{q}_A and \mathbf{q}_B . \mathbf{N}_g and \mathbf{N}_l are glued together to make \mathbf{N}_0 with an adjustable parameter, λ (0.1–1.5 by random selection). More details on the random mode generation and softening in SSW simulation can be found in our previous work.²⁴

$$\mathbf{N}_0 = \frac{\mathbf{N}_g + \lambda \mathbf{N}_l}{\|\mathbf{N}_g + \lambda \mathbf{N}_l\|}, \quad (2)$$

$$\mathbf{N}_l = (\dots, \mathbf{q}_A - \mathbf{q}_B, \dots, \mathbf{q}_B - \mathbf{q}_A, \dots). \quad (3)$$

2. SSW-RS method

The SSW-RS method searches the reaction space of a predefined minimum (reactant),^{22,24,29} i.e., searching for lowest barrier reaction pathways starting from specified reactants. It differs from the SSW method mainly in the structure selection module. Once a new minimum is reached in one SSW step, the acceptance probability P_r for a new minimum is decided according to a reaction criterion as described in Eq. (4). For molecular reactions, an obvious criterion is the bond connectivity: any breaking or forming of chemical bonds indicates the occurrence of a reaction, $P_r = 0$ in Eq. (2), and the new minimum will not be accepted. In this case ($P_r = 0$), we will record the structures of reactant and the new minimum (product) as a R/P reaction pair. By accumulating a large number of R/P pairs, the SSW-RS will sample effectively the reaction space for this reactant. After the SSW-RS simulation, the double-ended surface walking TS search²⁹ will be carried out using these R/P pairs (representing the reaction coordinate) to identify the lowest energy reaction channel,

$$P_r = \begin{cases} 0, & \text{reaction occurs} \\ 1, & \text{otherwise} \end{cases} \quad (4)$$

In SSW-RS, the local random mode \mathbf{N}_l in each SSW step may be replaced by a biased mode involving specific atoms learned from a target reaction pattern. This has been found to significantly speed up the search for the desired reaction space. For example, for a recombination reaction between CO and OH ($\text{CO} + \text{OH}$), a biased local mode \mathbf{N}_b describing the

reaction would be the vector [see Eq. (3)] between the C atom from CO and O atom from OH.

B. SSW-Cat method

The new SSW-Cat method intends to map out the lowest reaction pathway of heterogeneous catalytic reactions in an automated way. However, due to the large degrees of freedom in reaction, a fully automated search is highly computational demanding. To reduce the search space, the SSW-Cat implemented here will take advantage of the chemical knowledge, which provides a very basic description on the likely chemical identities of intermediates, the so-called reaction pattern. The overall algorithm is described as follows.

1. Algorithm

The flow chart for SSW-Cat is illustrated in Fig. 1(b), featuring with alternative SSW and SSW-RS simulations that are repeated for each minimum [or intermediate, **A**, **B**, and **C** in Fig. 1(b)] to cover all concerned reaction steps. The SSW simulation is performed for a limited number of SSW steps, \mathbf{n}_{SSW} , for each minimum, which helps to discover better configurations (e.g., different adsorption sites and different hydrogen bond networks). After the SSW structure search, starting from the current minimum, the SSW-RS with a fixed number of sampling steps, $\mathbf{n}_{\text{SSW-RS}}$, is then switched on to identify the likely reaction pathways. As shown in Fig. 1(b), by starting from **A** reactant, SSW-RS identifies a series of product minima \mathbf{B}_0 , \mathbf{B}_1 , \mathbf{B}_2 and thus generates a R/P database (i.e., $\mathbf{a}0/\mathbf{B}_0$, $\mathbf{a}1/\mathbf{B}_1$, and $\mathbf{a}2/\mathbf{B}_2$, where $\mathbf{a}0$, $\mathbf{a}1$, and $\mathbf{a}2$ are the conformation isomers for **A** reactant). Among these reactions, the product that matches the predefined reaction pattern, e.g., \mathbf{B}_0 in Fig. 1(b), will be taken to the next step as the minimum in the next SSW search. On the other hand, if a target reaction pattern is not found in the limited $\mathbf{n}_{\text{SSW-RS}}$ steps, SSW-Cat will return to one of the previous minima (using the saved configuration) to continue the search (for simplicity, the current implementation always returns back to the initial state). If all reaction steps are finished, SSW-Cat will not exit but return to the initial state, **A** in Fig. 1(b), to repeat the process.

While long simulation steps, \mathbf{n}_{SSW} and $\mathbf{n}_{\text{SSW-RS}}$, are desirable to identify the lowest energy pathway, it is in fact not necessary to set large \mathbf{n}_{SSW} and $\mathbf{n}_{\text{SSW-RS}}$ since the SSW-Cat is fully parallel and can be restarted from any intermediate. In this work, we typically run 20 SSW-Cat simulations in parallel and set both \mathbf{n}_{SSW} and $\mathbf{n}_{\text{SSW-RS}}$ as 5.

2. Reaction criterion

The success of SSW-Cat would rely on a robust criterion to judge whether a reaction occurs and whether a reaction occurred matches the target reaction pattern. In this work, we utilize multiple measures to guarantee a correct assessment for reaction.

First, the chemical bonding and the chirality are computed for each molecule/fragment. The chemical bonding is characterized by an $N \times N$ bond matrix in an N atom system. The corresponding matrix element is 1 if two atoms are bonded and is 0 if not. (The criterion for non-bonding is that the distance between two atoms exceeds the typical bond distance between

the two elements by 10%. For example, the bond matrix element is zero between O and H if their distance is more than 1.1 Å provided that the typical bond distance for O—H is 1.0 Å.)

Second, molecules (fragments) are also named according to the Simplified Molecular Input Line Entry System (SMILES),^{32,33} in which a molecule is represented by one unique notation regardless of the geometry conformation. The Open Babel package³⁴ is utilized to perform the conversion from Cartesian coordinates to SMILES text. Taking the reaction $\text{CO} + \text{H}_2\text{O} \rightarrow \text{CO}_2 + \text{H}_2$ as an example, the SMILES of this reaction can be represented as $[\text{C}]=\text{O} + \text{O} \rightarrow \text{O}=\text{C}=\text{O} + [\text{H}][\text{H}]$. For reactions on a solid surface, we disregard the solid surface, and only the Cartesian coordinate of molecules/adsorbates will be named using SMILES notation.

3. Reaction pattern

A reaction pattern needs to be defined first in the SSW-Cat search, which is used to bias (guide) the reaction search towards target reaction intermediates. While the reaction pattern represents in principle a reaction coordinate, it is possible to provide a simple description with basic chemical knowledge. The SSW-RS can code this simple description into an atomic displacement direction and refine it during the SSW search. A few parameters are taken as the input for the reaction pattern, which are used to generate a biased reaction mode \mathbf{N}_{rp} as written in Eq. (5). These include the atoms (or element types) that may form or break the chemical bond, a reaction cutoff radius r_{cut} , and a reaction selection probability λ_{rp} . In the equation, a random number (ran) in between (0,1) is compared with the reaction probability λ_{rp} , and the distance d between the two atoms is compared with r_{cut} .

$$\mathbf{N}_0 = \begin{cases} \frac{\mathbf{N}_g + \lambda \mathbf{N}_l}{\|\mathbf{N}_g + \lambda \mathbf{N}_l\|}, & \text{if } \text{ran} > \lambda_{\text{rp}} \text{ or } d > r_{\text{cut}} \\ \frac{\mathbf{N}_g + \lambda \mathbf{N}_{\text{rp}}}{\|\mathbf{N}_g + \lambda \mathbf{N}_{\text{rp}}\|}, & \text{if } \text{ran} < \lambda_{\text{rp}} \text{ and } d < r_{\text{cut}} \end{cases}. \quad (5)$$

For example, the reaction pattern for a CO + OH reaction on the surface is written as

$$\text{O1} \quad \text{C4} \quad 6.0 \quad 0.6 \quad 1. \quad (6)$$

O1 and C4 indicate the O atom in OH (atom index 1) and C atom in CO (atom index 4), respectively, from which we utilize Eq. (3) to generate a bond forming/breaking \mathbf{N}_{rp} between O1 and C4; the third number, 6.0, is r_{cut} , which indicates that O1 and C4 must be in a distance of 6.0 Å; the fourth number, 0.6, indicates the probability λ_{rp} that these two atoms are selected as the atom pair to react; the final number 1 stands for a bond forming mode between O1 and C4 (also see Sec. III A for reaction patterns).

C. Calculation details

1. Surface model

The Cu (111) surface is modeled by a (2×2) three layer slab, 4 Cu atoms per layer. The bottom two layers were kept fixed, and the top one layer was allowed to relax during the

SSW search. One CO and one H₂O molecule are initially added to the (2×2) Cu(111) surface as the starting point for SSW-Cat simulation.

2. DFT calculations

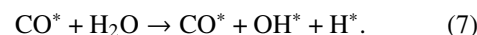
All SSW (including SSW-RS) simulations were carried out using SIESTA DFT package³⁵ with double- ζ polarization numerical atomic orbitals³⁶ and GGA-PBE³⁷ functional. To obtain more accurately the energetics for the reaction pathways, all structures (both minimum and TS) along the pathways reported here have been recalculated using plane-wave DFT VASP package.^{38,39} In VASP calculations, the kinetic energy cutoff was 400 eV, and the projector augmented wave (PAW) pseudopotential⁴⁰ was utilized to describe ionic core electrons. The exchange-correlation functional for DFT was GGA-PBE functional. A $(3 \times 3 \times 1)$ Monkhorst–Pack scheme⁴¹ was used for the first Brillouin zone k-point sampling. The geometry optimization convergence criterion in SSW simulations is 0.1 eV/Å for the maximal component of force, and this is reduced to 0.05 eV/Å in calculating the reaction pathways (including TS location).

III. RESULTS AND DISCUSSIONS

To demonstrate the ability of SSW-Cat in resolving the heterogeneous catalytic reaction network, we here utilize the water-gas shift reaction as an example, where CO reacts with H₂O on the Cu(111) surface. The overall reaction formula can be written as $\text{CO} + \text{H}_2\text{O} \rightarrow \text{CO}_2 + \text{H}_2$, occurring at temperatures above 473 K. CO₂/H₂ is the major product, but formic acid is suspected as an important intermediate.^{42–44} Water-gas shift reaction is of great importance in renewable energy generation and has been studied extensively both in experiment and in theory.^{43,45,46} After more than 40 years' studies, the reaction mechanism remains controversial, mainly on the nature of the intermediate formed, namely, formate (HCOO) and carboxyl (COOH) intermediates.

For the mechanism involving COOH, a three-step reaction pathway can be described as follows. Following the convention, we use the superscript * to indicate an adsorption state of molecule/fragment.

- (i) H₂O dissociation (breaking O—H bond):



- (ii) Carboxyl formation (forming C—O bond):



- (iii) CO₂ formation (breaking O—H bond):



(or $\text{COOH}^* + \text{H}^* \rightarrow \text{CO}_2 + \text{H}^* + \text{H}^*$).

It should be mentioned that the above mechanism cannot fully accommodate the production of formate or HCOOH during the water-gas shift reaction.^{47,48} The HCOOH formation is suspected to be the major channel at low temperatures (<400 K),⁴⁴ which might form via CO plus OH. Our aim in SSW-RS simulation is to identify the lowest energy pathway from CO/H₂O reactant to CO₂/H₂ product and in the meantime to resolve other minority reaction channels.

TABLE I. Statistics for SSW-Cat simulation to reveal the mechanism of water-gas shift reaction on Cu(111).

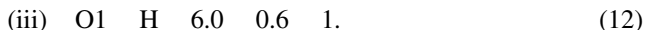
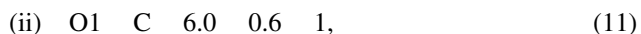
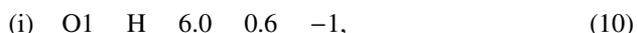
Reaction ^a	N _{SSW-RS} ^b	N _{Tot.}	N _{Path.}	N _{Path./N_{Tot.}} (%)	N _{Path./N_{SSW-RS}} (%)	Minimum barrier (eV)	Reaction energy (eV)
Step 1	12 619	1408	200	14.2	1.58	1.64	1.10
Step 2	2 446	171	42	24.6	1.71	0.40	0.20
Step 3	1 272	52	24	46.2	1.89	0.92	-0.14
Total	16 337	1631	266	16.3	1.62

^aStep 1: $\text{H}_2\text{O} \rightarrow \text{H}^* + \text{OH}^*$; Step 2: $\text{OH}^* + \text{CO}^* \rightarrow \text{COOH}^*$; Step 3: $\text{COOH}^* + \text{H}^* \rightarrow \text{CO}_2 + 2\text{H}^*$ (H_2).

^bN_{SSW-RS} is the total SSW steps in the SSW-RS; N_{Tot.} is the number of reaction pairs identified by SSW-RS, including both the target reaction and other branch channels; N_{Path.} is the number of the target reaction pairs.

A. Reaction patterns

The first step in SSW-Cat is to setup the reaction patterns that define the target reaction channel. Based on the general knowledge for water-gas reaction on Cu, the reaction steps (i) to (iii), we define the reaction patterns as follows.



Here O1 is the O atom in H_2O (OH). We do not specify a particular H atom in reaction, and thus only the element type (H) is supplied in the reaction pattern.

B. Overall efficiency of SSW-Cat

With the predefined reaction pattern, we then performed SSW-Cat simulation for $\text{CO} + \text{H}_2\text{O}$ reaction on Cu(111), which runs in 160 parallel jobs using 160 CPUs (20 cores per CPU). Table I summarized the statistics of SSW-Cat simulation. We terminated the simulation after 2065 minima in the SSW search, and 16 337 minima and 1631 R/P reaction pairs in SSW-RS were collected (see Table I). Each SSW step takes ~ 151 force/energy evaluation on average, and in total 2 482 456 force/energy evaluations (in 160 CPUs) were carried out using SIESTA.

By locating the TS for all these R/P pairs, we have determined the lowest energy pathway for the three steps and at the meantime identify several interesting branch reaction channels. The calculated reaction energies for the three reaction steps [reaction formulas (7)–(9)] are 1.10, 0.20, and -0.14 eV. The reaction barriers for the three steps following the reaction pattern in formulas (10)–(12) are 1.64, 0.40, and 0.92 eV. The first step, H_2O dissociation, is the rate-determining step.

Table I shows that for different reaction steps, the efficiency for the reaction sampling in SSW-RS is roughly the same, i.e., 1.5%–1.9%, being the ratio of the target reaction pathway in the total SSW-RS steps. In fact, the ratio for reaction in SSW-RS search is about 10% (the other 90% SSW steps belong to conformation change without molecular bond breaking/making), which means that $\sim 9\%$ reactions are not relevant to the reaction patterns in formulas (10)–(12).

It is interesting to compare the efficiency of unbiased reaction sampling for gas phase molecular reactions in our previous work,²⁴ where the ratio of the lowest reaction pathway in total SSW-RS steps is about 0.30%. The efficiency for

the surface reaction here is thus about 5 times higher, which can be attributed to the reaction patterns utilized in this work. These biased reaction modes speed up markedly the search towards the target reaction.

C. Thermodynamics and pathways

In Fig. 2, we show the reaction profile determined by SSW-Cat, in total 4 minima and three TSs (TS1 to TS3), together with the energy spectrum for each state. The four minima are initial state (IS) (CO^* and H_2O), intermediate state 1 (MS1) (CO^* , H^* , and OH^*), intermediate state 2 (MS2) (COOH^* and H^*), and final state (FS) (CO_2 , H^* , or H_2). The wide spread of the energy spectrum (typically 0.5 eV for both minimum and TS) indicates that many configurations are available for each state, which can now be resolved via SSW sampling.

To illustrate different configurational isomers, we also show the most stable conformation (indicated with letter a) and the second lowest stable conformation (indicated with letter b) for IS, MS1, and MS2 in Fig. 3(a). The hydrogen bonding network and the adsorption sites are two major factors in determining the stability of the structure. For the two IS structures (ISa and ISb) and the two MS1 structures (MS1a and MS1b), we found that the major difference is in the hydrogen bondings: the most stable structure ISa/MS1a has one more hydrogen

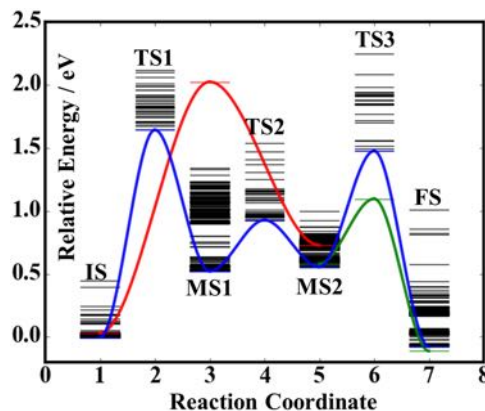


FIG. 2. Reaction energy profile for water-gas shift reaction revealed by the SSW-Cat search. The meaning of symbols are as follows. IS: CO^* and H_2O ; MS1: CO^* , H^* , and OH^* ; MS2: COOH^* and H^* ; FS: CO_2 , H^* , or H_2 . The energy spectrum for each state sampled from SSW is also plotted, which shows the presence of many energetically similar configurations for each state. The blue curve describes the lowest energy reaction profile for the target reactions; the red and green curves are the branch reaction channels described in Sec. III D. The green curve (formic acid formation) turns out to be the most kinetically favored pathway.

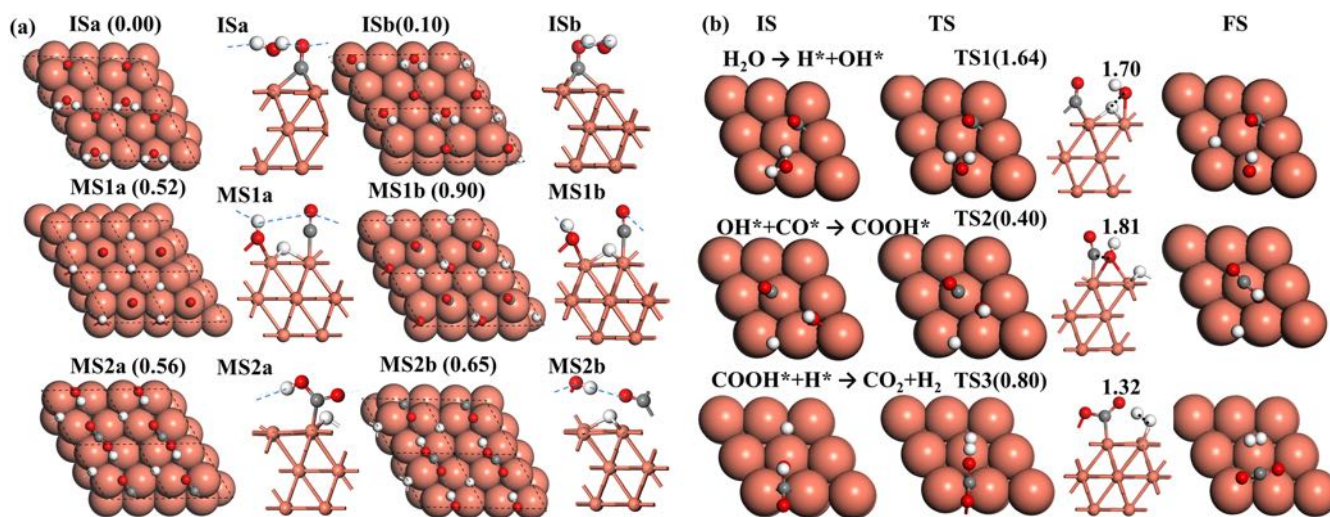


FIG. 3. Minima and pathways from SSW-Cat simulation. (a) Representative stable minima, including the top views (left) and side views (right). The letters *a* and *b* in each state (e.g., ISa and ISb) indicate the lowest energy minimum and the second lowest energy minimum, respectively, and the DFT energy of the state with respect to ISa is indicated in the parentheses. (b) Reaction snapshots along the identified lowest energy reaction pathways for the three-step mechanism from CO/H₂O to CO₂/H₂. From left to right are the IS, TS, and FS, respectively, and for the TS, a side view is also shown. Cu atom: large orange ball in the top view and small orange ball in the side view; H atom: small white ball; C atom: small grey ball; O atom: small red ball.

bond per unit cell than the less stable conformation. This leads to an energy difference of 0.38 eV between MS1a and MS1b. For MS2a and MS2b, while the number of hydrogen bonds is the same (one per unit cell), the location of adsorbed hydrogen atom differs. In MS2a, the hydrogen atom is at the fcc hollow site nearby the oxygen atom of COOH, whereas in the MS2b, the hydrogen is away from the O atom.

The reaction snapshots in the lowest energy pathway for the three-step mechanism from CO/H₂O to CO₂/H₂ are illustrated in Fig. 3(b), which are obtained by extrapolating the most stable TSs along the reaction direction. In the reaction, the water molecule first dissociates on a top site, while the CO nearby tends to form hydrogen bonding with the intact H of water ($\text{CO}^* \cdots \text{HO}^*$ 2.0 Å). In the second step, the CO recombines with the OH fragment to form a COOH, where the CO is at the top site and the OH sits at the bridge site at the TS. Finally, the COOH fragment reacts with the adsorbed H by losing its H. In the end, CO₂ and H₂ molecules are produced on the surface.

It might be mentioned that the lowest energy pathway connects the most stable minimum and the most stable TS, as outlined by blue curve in Fig. 2. However, the minima directly extrapolated from the most stable TS along the reaction direction may well not be the most stable minimum. For example, the most stable MS1 shown in Fig. 3 (MS1a) is slightly different from that (FS) extrapolated from TS1 in Fig. 3. In MS1a, the hydroxyl group adsorbs on the fcc hollow site, while in extrapolated MS1, the hydroxyl group is off a top site.

It is worth comparing our mechanism with the previous findings on water-gas shift reaction on Cu surfaces. Gokhale *et al.*⁴⁹ and Liu⁴³ show that the reaction barrier of the first step, H₂O dissociation, is 1.36–1.40 eV using GGA-PW91 and GGA-RPBE calculations with only one water molecule (no CO molecule) adsorbed on Cu (111). In our pathway, because an additional CO adsorbs nearby the water molecule (i.e., a

higher coverage), the calculated barrier is 1.64 eV, ~0.2 eV higher than the previous results. The obtained TS geometry is largely same, where H₂O dissociates on a top site of the Cu atom. Obviously, all these theoretical calculations confirm the experiment that water dissociation is the slowest step.⁵⁰ The reaction barrier for CO* + OH* was computed to be 0.61 eV with reference to well-separated CO and OH and 0.35 eV referred to co-adsorbed CO and OH (using GGA-PW91),^{43,49} which is consistent with our value (0.40 eV using GGA-PBE).

Interestingly, our results show that the third step, CO₂ formation, is quite facile with only a barrier of 0.92 eV, 0.72 eV lower than the first step. However, Gokhale *et al.*⁴⁹ reported a barrier of 1.41 eV for COOH dissociation on Cu (111). While their pathway produces the adsorbed H atom on the surface, our new mechanism shows that the H transfer from COOH to the adsorbed H is kinetically more feasible: the CO₂ formation and H₂ formation can occur in one elementary step. This result illustrates well the ability of SSW-Cat for the discovery of new reaction mechanism (Fig. 4).

It should be mentioned that SSW-Cat also identifies the COOH direct dissociation pathway, which is indeed kinetically more difficult. In Fig. 5, we compare different pathways for COOH dissociation to produce CO₂. Pathway 1 (blue curve) is the one ($\text{COOH} + \text{H} \rightarrow \text{CO}_2 + \text{H}_2$) shown in Fig. 3, having the lowest barrier. Pathway 2 (solid black curve) is the direct dissociation of COOH ($\text{COOH}^* + \text{H}^* \rightarrow \text{CO}_2 + 2\text{H}^*$) with a nearby adsorbed H atom. Pathway 3 (dotted black curve) is the direct dissociation of COOH on a bare Cu(111), a model same with that used previously.⁴³ We found that (i) pathway 1 is the kinetically preferred pathway among the three possibilities. The final state, CO₂ and H₂, is in fact less stable than the final state in pathway 2, CO₂ with two adsorbed H atoms because the dissociative adsorption of H₂ is exothermic. (ii) The high coverage of H (pathway 2) helps to stabilize the TS structure by 0.15 eV and thus reduce the reaction barrier.

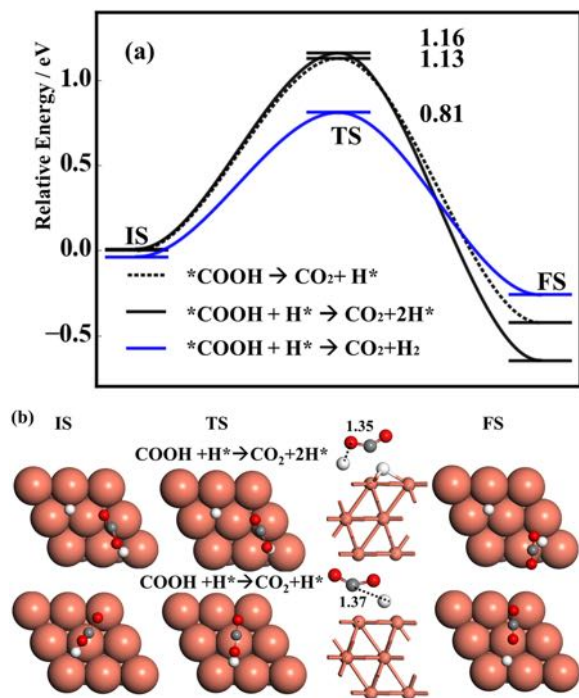


FIG. 4. (a) Reaction energy profiles for three different COOH dehydrogenation pathways to form CO₂. The energy of coadsorbed COOH* and H* in a 2 × 2 supercell is set as the energy zero reference. (b) The reaction snapshots for COOH* → CO₂ + H* [dotted black curve in (a)] and COOH* + H* → CO₂ + 2H* [solid black curve in (a)]. The reaction snapshots for the lowest energy pathway (blue curve), COOH* + H* → CO₂ + H₂, are shown in Fig. 3.

D. Branch reaction channels

Apart from the target reaction pathway guided by the predefined reaction patterns, SSW-Cat can reveal other reaction channels sharing the same reaction intermediates. As shown in Table I, for each minimum, there is in fact ~90% probability to explore the branch reactions that do not match with the target reaction pattern. By locating the TS of these pathways, it is possible to identify unexpected reaction channels. In this work, we have analyzed all the branch pathways, in total 283 R/P pairs. From them, we identify two interesting branching reactions that are numbered as (iv) and (v) in addition to (i-iii) reactions in the target route.

(iv) Concerted COOH formation:



(v) Formic acid formation by carboxyl hydrogenation:



The energy profiles of these two pathways are shown in Fig. 2 (red and green curves), and their reaction snapshots are shown in Fig. 5. Below we discuss them in more detail.

1. $\text{H}_2\text{O} + \text{CO}^* \rightarrow \text{H}^* + \text{COOH}^*$

Different from the stepwise mechanism via H₂O dissociation and CO/OH recombination, SSW-Cat finds a concerted pathway to form COOH from H₂O and CO directly, which has been proposed in the literature.⁵¹ The reaction involves a concerted TS where the HO—H bond breaking occurs simultaneously with the OC···OH bond formation. At the TS, H₂O

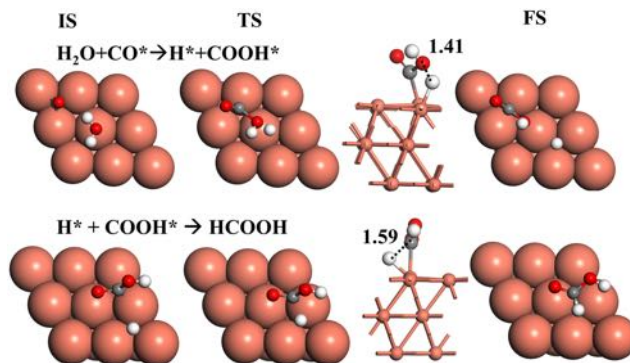


FIG. 5. Reaction snapshots for two branch reaction channels: a concerted reaction (top panel) to produce carboxyl (also see the red curve in Fig. 2) and a carboxyl hydrogenation (bottom panel) pathway to form formic acid (also see the green curve in Fig. 2).

sits at a top site and CO is off a nearby top site [see Fig. 5(a)]. The reaction barrier for this concerted pathway is very high, 2.02 eV, with respect to the most stable IS. It is thus concluded that the stepwise mechanism via COOH intermediate shown in Fig. 2 is kinetically much preferable than a one-step reaction.

2. $\text{H}^* + \text{COOH}^* \rightarrow \text{HCOOH}$

Instead of carboxyl dehydrogenation in the step 3, it is likely for COOH to react with a nearby H to form formic acid. At the located TS for this reaction, the COOH and H move close to share bonding with the same Cu atom. After the reaction, HCOOH desorbs and lies flat over the surface.

Importantly, the reaction barrier for the hydrogenation of COOH pathway is only 0.51 eV. This is considerably lower than the carboxyl dehydrogenation to form CO₂. This new finding implies that the formic acid formation is kinetically much preferable than the CO₂ formation.

The previous computational study by Gokhale *et al.*⁴⁹ missed the H* + COOH* pathway and they suggested that HCOOH and formate, major intermediates at low temperature experiments,⁴⁸ are produced from the direct CO₂ hydrogenation, which however has a very high barrier, 1.02 eV from DFT. Our results show, reversely, that formic acid is produced from COOH hydrogenation and formate should be the dehydrogenation product from formic acid. Our conclusion is consistent with the recent experimental study that formate formation from HCOOH starts as early as 160 K.⁵²

E. Discussions on the overall mechanism for water-gas shift on Cu

With all the kinetics data from SSW-Cat simulation, we are now at the position to discuss the overall mechanism of water-gas shift reaction on Cu(111). While H₂O dissociation with 1.64 eV barrier is undoubtedly the rate-determining step for the reaction on Cu(111), the product selectivity appears to be sensitive to the H coverage. In the absence of H, COOH will break its O—H bond to form CO₂ and adsorbed H atoms. The H₂ molecule can be released later via the recombination of adsorbed H atoms. The calculated barrier for H atom recombination is >1.0 eV.^{53,54} On the other hand, in the presence of

nearby adsorbed H, the HCOOH formation becomes kinetically much preferable: the barrier of $\text{COOH}^* + \text{H}^* \rightarrow \text{HCOOH}$ is only 0.51 eV, which is 0.33 eV lower than the lowest barrier channel of CO_2 formation ($\text{COOH}^* + \text{H}^* \rightarrow \text{CO}_2 + \text{H}_2$). It is therefore necessary to know the H coverage under experimental conditions in order to determine which reaction channel is kinetically favored.

Considering that the diffusion barrier of H on the Cu surface is much lower (0.15 eV⁵⁵) than that from all bond making/breaking reactions, the much higher barrier for H—H coupling (1.0 eV) than that of HCOOH formation (0.51 eV) means that the major H consumption channel is via the $\text{COOH}^* + \text{H}^*$ reaction to form HCOOH. For the low barrier in H consumption (0.5 eV), it is expected that the H coverage on the surface is hard to build up, and the formation of HCOOH and the subsequent formate formation via HCOOH dehydrogenation should be the major reaction channel in water-gas shift reaction. By elevating temperatures, HCOOH and formate will further decompose to release CO_2 and H_2 because CO_2 and H_2 are thermodynamically more favorable due to the entropy contribution at high temperatures. The reaction equilibrium therefore shifts towards the CO_2 and H_2 products. This has been indeed observed recently in experiment. Marcinkowski *et al.* by performing surface science studies for formic acid decomposition on Cu(111) showed that at 160 K the adsorbed HCOOH will become formate and H on the surface. Further increasing the temperature to 450 K, the formate will finally convert to CO_2 and H_2 is also produced by H—H coupling.⁵²

It should be emphasized that formate as an intermediate for water-gas shift reaction on Cu has been suggested in experiment since 1980s.^{47,51,56,57} The formate pathway was proposed via $\text{CO}^* + \text{OH}^* \rightarrow \text{HCOO}^*$, which however turns out to be not favored energetically according to DFT calculations. Instead, theory reveals that $\text{CO}^* + \text{OH}^*$ prefers to form carboxyl^{58–60} although COOH^* is never observed in experiment. To reconcile with experimental evidences on the formate intermediate, it was proposed that formate might alternatively form via CO_2 direct hydrogenation, which is hindered by a high barrier from DFT (>1 eV) and thus is apparently contradictory with the low temperature observation of formate. Using SSW-Cat, we reconcile this puzzle. We show that COOH^* can readily hydrogenate to form HCOOH, which is known to decompose into formate at low temperatures (160 K).

IV. CONCLUDING REMARKS

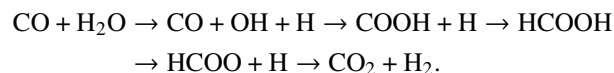
This work represents our latest effort in developing an efficient computational approach for automated structure and reaction prediction. The new SSW-Cat method pushes the limit to heterogeneous catalytic reactions, where the intermediates and reaction pathways are rich, many beyond the current knowledge framework. The SSW-Cat utilizes the SSW global optimization method to explore all the likely conformation isomers of intermediates. The conversion between these conformers is rapid, and thus the explicit reaction pathway location is not essential; the SSW-Cat then utilizes the SSW-RS to explore the reaction space for (suspected) key intermediates, which helps to determine the lowest energy reaction

pathway for the slow reaction steps involving chemical bond making/breaking. This manual separation of reactions in the time domain and the utilization of global optimization methods allow us to quickly identify the reaction mechanism, including the rate-determining step and the major reaction intermediate.

Taking a well-studied heterogeneous catalytic reaction as an example, i.e., water-gas shift reaction on a simple close-packed surface, Cu(111), we utilize massively parallel SSW-Cat simulation to revisit the reaction mechanism. The SSW-Cat confirms the water dissociation as the rate-determining step and reveals a new mechanism for formic acid formation. In the current implementation, we provide a target reaction pattern that is generally available from basic chemical knowledge to guide the SSW-Cat search, which is the only information required in simulation. For the water-gas shift reaction, we show that even this initial information is not perfect, the SSW-Cat can help to rule out the pre-set three-step mechanism,

$$\text{CO} + \text{H}_2\text{O} \rightarrow \text{CO} + \text{OH} + \text{H} \rightarrow \text{COOH} + \text{H} \rightarrow \text{CO}_2 + \text{H}_2,$$

but suggest a five-step alternative,



It is concluded that formic acid is facile to produce from carboxyl (barrier 0.51 eV) and acts as the major intermediate together with carboxyl and formate.

As a successful practice of combining SSW and SSW-RS, the SSW-Cat holds the promise for resolving in general the reaction network of complex heterogeneous catalytic reaction on the surface and interfaces, such as Fischer–Tropsch reaction.^{61,62} The simultaneous treatment of structure and reaction degrees of freedom via SSW global optimization could be a solution towards clarifying challenging catalytic chemistry.

ACKNOWLEDGMENTS

This work is supported by the National Science Foundation of China (Grant No. 21533001), 973 Program (No. 2013CB834603), and Science and Technology Commission of Shanghai Municipality (Grant No. 08DZ2270500).

¹G. Ertl, S. B. Lee, and M. Weiss, *Surf. Sci.* **114**(2), 527 (1982).

²Z.-P. Liu, S. J. Jenkins, and D. A. King, *Phys. Rev. Lett.* **94**(19), 196102 (2005).

³B. Hammer and J. K. Nørskov, *Adv. Catal.* **45**, 71 (2000).

⁴Z. W. Ulissi, A. J. Medford, T. Bligaard, and J. K. Nørskov, *Nat. Commun.* **8**, 14621 (2017).

⁵A. Alavi, P. Hu, T. Deutsch, P. L. Silvestrelli, and J. Hutter, *Phys. Rev. Lett.* **80**(16), 3650 (1998).

⁶G.-J. Cheng, X. Zhang, L. W. Chung, L. Xu, and Y.-D. Wu, *J. Am. Chem. Soc.* **137**(5), 1706 (2015).

⁷D. J. Wales, *Int. Rev. Phys. Chem.* **25**(1-2), 237 (2006).

⁸G. Henkelman and H. Jónsson, *J. Chem. Phys.* **111**(15), 7010 (1999).

⁹G. Henkelman, B. P. Uberuaga, and H. Jónsson, *J. Chem. Phys.* **113**(22), 9901 (2000).

¹⁰H.-F. Wang and Z.-P. Liu, *J. Am. Chem. Soc.* **130**(33), 10996 (2008).

¹¹C. Shang and Z.-P. Liu, *J. Chem. Theory Comput.* **6**(4), 1136 (2010).

¹²R. Martoňák, D. Donadio, A. R. Oganov, and M. Parrinello, *Nat. Mater.* **5**(8), 623 (2006).

¹³D. J. Wales, *Mol. Phys.* **100**(20), 3285 (2002).

¹⁴B. Schaefer, S. Mohr, M. Amsler, and S. Goedecker, *J. Chem. Phys.* **140**(21), 214102 (2014).

- ¹⁵D. J. Wales, *J. Chem. Phys.* **130**(20), 204111 (2009).
- ¹⁶L. Xu and G. Henkelman, *J. Chem. Phys.* **129**(11), 114104 (2008).
- ¹⁷S. Maeda, S. Komagawa, M. Uchiyama, and K. Morokuma, *Angew. Chem., Int. Ed.* **50**(3), 644 (2011).
- ¹⁸R. Ramozzi and K. Morokuma, *J. Org. Chem.* **80**(11), 5652 (2015).
- ¹⁹S. Maeda, K. Ohno, and K. Morokuma, *Phys. Chem. Chem. Phys.* **15**(11), 3683 (2013).
- ²⁰C. F. Goldsmith and R. H. West, *J. Phys. Chem. C* **121**(18), 9970 (2017).
- ²¹S. Rangarajan, A. Bhan, and P. Daoutidis, *Comput. Chem. Eng.* **45**, 114 (2012).
- ²²C. Shang and Z. P. Liu, *J. Chem. Theory Comput.* **9**(3), 1838 (2013).
- ²³X. J. Zhang, C. Shang, and Z. P. Liu, *J. Chem. Theory Comput.* **9**(7), 3252 (2013).
- ²⁴X.-J. Zhang and Z.-P. Liu, *Phys. Chem. Chem. Phys.* **17**(4), 2757 (2015).
- ²⁵H.-J. Zhai, Y.-F. Zhao, W.-L. Li, Q. Chen, H. Bai, H.-S. Hu, Z. A. Piazza, W.-J. Tian, H.-G. Lu, and Y.-B. Wu, *Nat. Chem.* **6**(8), 727 (2014).
- ²⁶G.-F. Wei and Z.-P. Liu, *J. Chem. Theory Comput.* **12**(9), 4698 (2016).
- ²⁷S.-C. Zhu, S.-H. Xie, and Z.-P. Liu, *J. Am. Chem. Soc.* **137**(35), 11532 (2015).
- ²⁸S.-H. Guan, X.-J. Zhang, and Z.-P. Liu, *J. Am. Chem. Soc.* **137**(25), 8010 (2015).
- ²⁹X.-J. Zhang, C. Shang, and Z.-P. Liu, *J. Chem. Theory Comput.* **9**(12), 5745 (2013).
- ³⁰Q. Chen, G.-F. Wei, W.-J. Tian, H. Bai, Z.-P. Liu, H.-J. Zhai, and S.-D. Li, *Phys. Chem. Chem. Phys.* **16**(34), 18282 (2014).
- ³¹X.-J. Zhang, C. Shang, and Z.-P. Liu, *Phys. Chem. Chem. Phys.* **19**(6), 4725 (2017).
- ³²D. Weininger, *J. Chem. Inf. Model.* **28**(1), 31 (1988).
- ³³D. Weininger, A. Weininger, and J. L. Weininger, *J. Chem. Inf. Model.* **29**(2), 97 (1989).
- ³⁴A. Karwath and L. De Raedt, *J. Chem. Inf. Model.* **46**(6), 2432 (2006).
- ³⁵M. S. José, A. Emilio, D. G. Julian, G. Alberto, J. Javier, O. Pablo, and S.-P. Daniel, *J. Phys.: Condens. Matter* **14**(11), 2745 (2002).
- ³⁶J. Junquera, Ó. Paz, D. Sánchez-Portal, and E. Artacho, *Phys. Rev. B: Condens. Matter Mater. Phys.* **64**(23), 235111 (2001).
- ³⁷J. P. Perdew, K. Burke, and M. Ernzerhof, *Phys. Rev. Lett.* **77**(18), 3865 (1996).
- ³⁸G. Kresse and J. Hafner, *Phys. Rev. B: Condens. Matter Mater. Phys.* **47**(1), 558 (1993).
- ³⁹G. Kresse and J. Furthmüller, *Comput. Mater. Sci.* **6**(1), 15 (1996).
- ⁴⁰G. Kresse and D. Joubert, *Phys. Rev. B: Condens. Matter Mater. Phys.* **59**(3), 1758 (1999).
- ⁴¹H. J. Monkhorst and J. D. Pack, *Phys. Rev. B: Condens. Matter Mater. Phys.* **13**(12), 5188 (1976).
- ⁴²Y. Yasaka, K. Yoshida, C. Wakai, N. Matubayasi, and M. Nakahara, *J. Phys. Chem. A* **110**(38), 11082 (2006).
- ⁴³P. Liu, *J. Chem. Phys.* **133**(20), 204705 (2010).
- ⁴⁴A. E. Baber, K. Mudiyansele, S. D. Senanayake, A. Beatriz-Vidal, K. A. Luck, E. C. H. Sykes, P. Liu, J. A. Rodriguez, and D. J. Stacchiola, *Phys. Chem. Chem. Phys.* **15**(29), 12291 (2013).
- ⁴⁵A. B. Vidal and P. Liu, *Phys. Chem. Chem. Phys.* **14**(48), 16626 (2012).
- ⁴⁶J. A. Rodriguez, J. Graciani, J. Evans, J. B. Park, F. Yang, D. Stacchiola, S. D. Senanayake, S. Ma, M. Pérez, P. Liu, J. F. Sanz, and J. Hrbek, *Angew. Chem., Int. Ed.* **48**(43), 8047 (2009).
- ⁴⁷D. C. Grenoble, M. M. Estadt, and D. F. Ollis, *J. Catal.* **67**(1), 90 (1981).
- ⁴⁸I. Fishtik and R. Datta, *Surf. Sci.* **512**(3), 229 (2002).
- ⁴⁹A. A. Gokhale, J. A. Dumesic, and M. Mavrikakis, *J. Am. Chem. Soc.* **130**(4), 1402 (2008).
- ⁵⁰J. Nakamura, J. M. Campbell, and C. T. Campbell, *J. Chem. Soc., Faraday Trans.* **86**(15), 2725 (1990).
- ⁵¹D. S. Newsome, *Catal. Rev.* **21**(2), 275 (1980).
- ⁵²M. D. Marcinkowski, C. J. Murphy, M. L. Liriano, N. A. Wasio, F. R. Lucci, and E. C. H. Sykes, *ACS Catal.* **5**(12), 7371 (2015).
- ⁵³M. J. Murphy and A. Hodgson, *J. Chem. Phys.* **108**(10), 4199 (1998).
- ⁵⁴A. Forni, G. Wiesenekker, E. J. Baerends, and G. F. Tantardini, *Int. J. Quantum Chem.* **52**(4), 1067 (1994).
- ⁵⁵J. Greeley and M. Mavrikakis, *J. Phys. Chem. B* **109**(8), 3460 (2005).
- ⁵⁶T. van Herwijnen and W. A. de Jong, *J. Catal.* **63**(1), 83 (1980).
- ⁵⁷T. van Herwijnen, R. T. Guzcalski, and W. A. de Jong, *J. Catal.* **63**(1), 94 (1980).
- ⁵⁸Q.-L. Tang, Q.-J. Hong, and Z.-P. Liu, *J. Catal.* **263**(1), 114 (2009).
- ⁵⁹Q.-L. Tang and Z.-P. Liu, *J. Phys. Chem. C* **114**(18), 8423 (2010).
- ⁶⁰Q.-J. Hong and Z.-P. Liu, *Surf. Sci.* **604**(21), 1869 (2010).
- ⁶¹J. Chen and Z.-P. Liu, *J. Am. Chem. Soc.* **130**(25), 7929 (2008).
- ⁶²G. L. Bezemer, J. H. Bitter, H. P. C. E. Kuipers, H. Oosterbeek, J. E. Holewijn, X. Xu, F. Kapteijn, A. J. van Dillen, and K. P. de Jong, *J. Am. Chem. Soc.* **128**(12), 3956 (2006).